analytical chemistry

Article

pubs.acs.org/ac

Sensitive, Simultaneous Quantitation of Two Unlabeled DNA Targets Using a Magnetic Nanoparticle–Enzyme Sandwich Assay

Yue Zhang,[†] Chalermchai Pilapong,[†,∥] Yuan Guo,*[,†] Zhenlian Ling,[†] Oscar Cespedes,[‡] Philip Quirke,[§] and Dejian Zhou*[,†]

[†]School of Chemistry and Astbury Centre for Structural Molecular Biology, University of Leeds, Leeds LS2 9JT, U.K.

[‡]School of Physics and Astronomy, University of Leeds, Leeds, LS2 9JT, U.K.

[§]Section of Pathology and Tumour Biology, Leeds Institute of Molecular Medicine, Wellcome Trust Brenner Building, St. James's University Hospital, University of Leeds, Leeds LS9 7TF, U.K.

Supporting Information

ABSTRACT: We report herein the development of a simple, sensitive colorimetric magnetic nanoparticle (MNP)–enzyme-based DNA sandwich assay that is suitable for simultaneous, label-free quantitation of two DNA targets down to 50 fM level. It can also effectively discriminate single-nucleotide polymorphisms (SNPs) in genes associated with human cancers (KRAS codon 12/13 SNPs). This assay uses a pair of specific DNA probes, one being covalently conjugated to an MNP for target capture and the other being linked to an enzyme for signal amplification, to sandwich a DNA target, allowing for convenient magnetic separation and subsequent efficient enzymatic signal amplification for high sensitivity. Careful optimization of the MNP surfaces and assay conditions greatly reduced the background, allowing for sensitive, specific detection of as little as 5 amol (50 fM in 100 μL) of target DNA. Moreover, this sensor is robust, it can effectively discriminate cancer-specific SNPs against the wild-type noncancer target, and it works efficiently in 10% human serum. Furthermore, this sensor can simultaneously quantitate two different DNA targets by using two pairs of unique capture- and signal-DNA probes specific for each target. This general, simple, and sensitive DNA sensor appears to be well-suited for a wide range of genetics-based biosensing and diagnostic applications.

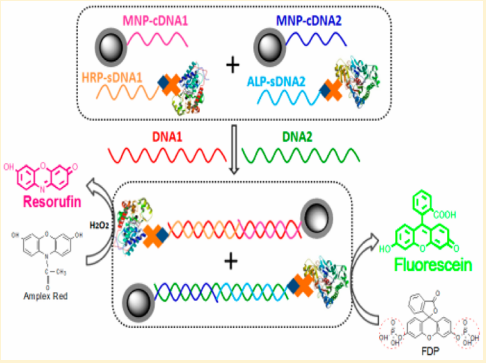

The development of biosensors capable of rapid, sensitive detection of specific genetic biomarkers is critical to health care, allowing diagnosis of diseases, prediction of patients' responses to treatment, and risk of relapse of disease.[1,2] The polymerase chain reaction (PCR) is the most widely used technique for DNA detection due to its great, exponential amplification capability.[3] However, as a paradox of its great amplification power, even a tiny amount of contaminant can result in a non-negligible false positive which can affect diagnostic accuracy. Moreover, PCR requires a relatively clean lab environment and long assay period, making it less well-suited for rapid, on-site diagnosis. Therefore, alternative, PCR-free based DNA sensing approaches have been actively exploited over the past decade, among which, several gold nanoparticle (GNP)-based methods, e.g., silver-amplified scannometric assay,[4] silver-amplified electric detection,[5] silver-amplified Raman finger printing,[6] and magnetic microparticle-assisted DNA nanobarcode assay,[7] have exhibited exceptional promise. They displayed excellent sensitivities and specificities for DNA detection, down to the femtomole per liter to attomole per liter level, making them potentially suitable for direct target detection without the need of PCR preamplification. Despite these, most assays use surface-immobilized DNA probes for soluble target capture, a heterogeneous process that often suffers from slow binding kinetics and low capture efficiency. As a result, a relatively long period for target capture and GNP sandwich binding (ca. 6–8 h) is required,[4−6] making them less well-suited for rapid detection.

Meanwhile, functional nanoparticles, such as quantum dots, metal nanoparticles, and magnetic nanoparticles (MNPs), have unique, size-dependent optical and electrical properties that are well-suited for biosensing. In this regard, MNPs are extremely well-suited because of several attractive properties, e.g., ease of synthesis, versatile surface modification strategies, good stability, low toxicity, and moreover their superparamagnetic properties. As a result, they form stable, uniform dispersions in the media for homogeneous, rapid, and efficient target capture without an external magnetic field, but are readily collected and separated from the media upon applying an external magnetic field. Moreover, a large excess of MNP capture probes can be used to push the equilibrium of the target–probe binding toward the captured state, allowing efficient target detection at concentrations far below the equilibrium dissociation constant

Received: June 28, 2013
Accepted: August 26, 2013
Published: August 26, 2013

   dx.doi.org/10.1021/ac402081u | *Anal. Chem.* 2013, 85, 9238–9244

(K_d).[7,8] These make them extremely well-suited for biosensing, bioseparation, and biocatalysis. Meanwhile, enzymes are extremely versatile, efficient biocatalysts with great substrate turnover (signal amplification) power, making them attractive for ultrasensitive biosensing. In fact, some of most widely used commercial diagnostic assays, e.g., the enzyme-linked immunosorbent assay (ELISA), are based on enzymes such as horseradish peroxidase (HRP) and alkaline phosphatase (ALP). Enzymes have been combined with electrochemical, electrochemiluminescence, colorimetric, and fluorimetric readout strategies in sensing, among which, electrochemical readout is widely used in point-of-care (PoC) diagnostics (e.g., the famous personal glucose meter).[9] Despite high convenience, such PoC diagnostics are mostly suitable for highly abundant targets due to limited sensitivity (e.g., micromoles per liter to millimoles per liter). For early diagnosis, a much higher sensitivity is needed.[1,2] Furthermore, most DNA sensors have been demonstrated with a single target, which can limit diagnostic accuracy because "*no tumor marker identified to date is sufficiently sensitive or specific to be used on its own to screen for cancer*".[10] Therefore, the ability of detecting multiple analytes simultaneously is important to high diagnostic accuracy. In this regard, several multiplexed biodetection methods have been reported, including the giant magnetoresistive (GMR) sensor,[11] multicolor GNP surface-enhanced Raman spectroscopy (SERS) fingerprinting,[6] GNP multicolor nanobeacons,[1] multicolor molecular beacons (MBs),[12] and graphene quenched multicolor sensors.[13] Nevertheless, the sensitivity of most approaches (e.g., high picomole per liter to low nanomole per liter for the latter three) needs to be improved considerably to make them competitive against existing clinical diagnostic assays. By combining the advantageous properties of both MNP and enzymes, here we have developed a simple, sensitive MNP−enzyme sandwich assay suitable for label-free quantitation of two DNA targets. We show this sensor is sensitive (50 fM), robust (works in 10% human serum), and specific (can efficiently discriminate cancer-specific single-base mutants from the wild-type noncancer target).

EXPERIMENTAL SECTION

Materials. HPLC-purified DNA probes and target strands were purchased commercially from the IBA GmbH (Germany). Their sequences are given in Table 1. HRP−neutravidin (HRP−NAV) and ALP−neutravidin (ALP−NAV) conjugates were purchased from Thermo Scientific (U.K.). Amplex red and fluorescein diphosphate (FDP) were purchased from Invitrogen Life Technologies (U.K.). The heterofunctional cross-linker SM(PEG)$_{12}$ was purchased from Fisher Scientific Ltd. (U.K.). All other chemicals and reagents were purchased from Sigma-Aldrich (U.K.). PBS (137 mM NaCl, 10 mM Na_2HPO_4, 2.7 mM KCl, and 1.8 mM KH_2PO_4, pH 7.4) and Tris buffer (100 mM Tris·HCl, 100 mM NaCl, pH 8.5) were made with ultrapure Milli-Q water (resistance >18 MΩ·cm^{-1}). The MNPs were synthesized and modified in-house (see the Supporting Information for details).

Table 1. DNA Sequences and Their Abbreviations[a]

name	sequence (5′ → 3′)
cDNA1	HS−TTT TTT TCC GAC CTG GGG
sDNA1	GAG TAT TGC GGA GGA TTT TTT−biotin
T-DNA1	TCC TCC GCA ATA CTC CCC CAG GTC GGA
cDNA2	HS−TTT TTT GGC AGT CCG TGG TAG
sDNA2	GGC AGG TTG GGG TGA TTT TTT−biotin
T-DNA2	TCA CCC CAA CCT GCC CTA CCA CGG ACT GCC
cDNA3	TGG CGT AGG CAA GAG TTT TTT TTT TT−HS
sDNA3	biotin−TTT TTT GTG GTA GTT GGA GCT GG
T-DNA3	ACT CTT GCC TAC GCC A**C**C AGC TCC AAC TAC CAC
T-DNA4	ACT CTT GCC TAC GCC A***T***C AGC TCC AAC TAC CAC
T-DNA5	ACT CTT GCC TAC GCC A***A***C AGC TCC AAC TAC CAC

[a]T-DNA4 and T-DNA5 are two cancer-specific single-base mutants of the KRAS codon 12/13, while T-DNA3 is the wild-type target.

Instruments. UV−vis spectra were recorded on a Cary 50 Bio UV−vis spectrophotometer with 1.0 cm optical path length.[15] The spectra were corrected by their respective buffer background. The HRP-based DNA detection limit assay was monitored by fluorescence time trace on an Envision plate reader using BODIPY TMR FP 531 as excitation filter and Cy3 595 as emission filter.[18] The powder X-ray diffractogram was performed on PANalytical's X'Pert PRO materials research diffractometer (MRD) using a scan range (2θ) of 10−90° at increments of 0.0332°. The magnetization measurement was carried out on a MagLab vibration sample magnetometer (Oxford Instruments) at 55 Hz with amplitude of 1.5 mm. The samples were measured at room temperature (RT) at a scan rate of 9.17 mT·s^{-1}.[15a]

General Assay Procedure. The capture DNAs (cDNAs) were covalently conjugated to amine-modified MNPs via a heterofunctional cross-linker SM(PEG)$_{12}$ (Supporting Information). The PEGylated cross-linker is used because it can effectively resist nonspecific adsorption,[25] greatly reducing background. The cDNA loading on the MNP was estimated by our previous method.[18] The signal DNA (sDNA) was linked to neutravidin (NAV), HRP, or ALP conjugate via the strong biotin−NAV interaction at 1:1 molar ratio.[15] For a typical UV−vis assay, MNP−cDNA (20 μg), HRP−sDNA (5 pmol), and various amounts of T-DNA were mixed to make a series of samples (final volume: 500 μL in PBS containing 1 mg/mL BSA). After incubation for 1 h at RT, the MNP−dsDNA−En sandwiches were separated magnetically and the clear supernatants were discarded. The MNPs were washed with PBS once, PBS with 0.1% Tween-20 twice, and finally PBS once again to remove any unbound species. The MNP sandwiches were then dispersed in PBS (380 μL), and enzymatic amplification was initiated by adding Amplex red/H_2O_2 (50 μL each, both 0.2 mM). After a certain period, 20 μL of N_3Na (1 M) was added to stop further amplification and the UV−vis spectra of the supernatants were recorded.

For ALP-based assay, the procedures were the same as above, except where sDNA2−ALP and FDP were used. All assays and washing steps were performed in Tris buffer. The termination of enzyme amplification was achieved by adding 20 μL of PBS to the assay solution. For simultaneous quantitation of two DNA targets, the whole assay was carried out in Tris buffer using a mixture of MNP−cDNA1 and MNP−cDNA2 (15 μg each). After sandwich binding and washing steps, FDP and Amplex red were added simultaneously to initiate enzymatic amplifications. All other assay details are given in the Supporting Information.

RESULTS AND DISCUSSION

The principle of the MNP−enzyme sandwich assay for simultaneous detection of two T-DNAs is shown schematically in Scheme 1. Two sets of unique MNP-capture and En-signal probes are used to target two specific T-DNAs (e.g., MNP−

dx.doi.org/10.1021/ac402081u | Anal. Chem. 2013, 85, 9238−9244

Scheme 1. Principle of the MNP−Enzyme Sandwich Assay for Simultaneous Detection of Two DNA Targets Using Two Sets of Unique MNP−cDNA and sDNA−En Probes[a]

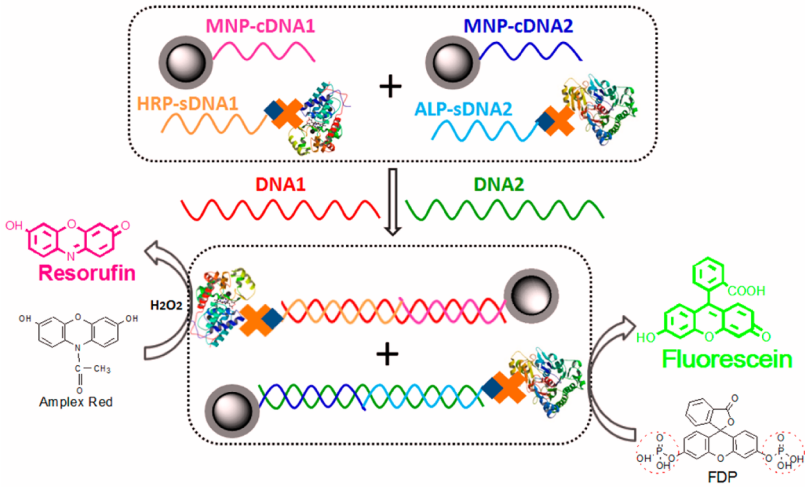

[a]The cDNA and sDNA probes are complementary to each half of their DNA targets for specific sandwich hybridization, linking HRP (with T-DNA1) or ALP (with T-DNA2) to the MNP. Therefore, HRP/ALP-amplified enzyme products, resorufin (λ_{max} = 571 nm) and fluorescein (λ_{max} = 485 nm), are used to quantitate T-DNA1/T-DNA2, respectively.

cDNA1/HRP−sDNA1 for T-DNA1; MNP−cDNA2/ALP−sDNA2 for T-DNA2). In the presence of T-DNA1, HRP−sDNA1 will bind to MNP−cDNA1 via specific sandwich hybridization, while T-DNA2 will link ALP−sDNA2 to MNP−cDNA2. All these are performed in homogeneous solutions, allowing for efficient, rapid T-DNA capture and conversion of each captured T-DNA1 or T-DNA2 into an HRP or ALP for signal amplification. A large excess of MNP−cDNA and sDNA−En probes (10−200 000-fold molar equivalent of T-DNA, depending on T-DNA concentration) is used to push the equilibrium of the MNP−cDNA/T-DNA/sDNA−En sandwich hybridization toward the hybridized state. A high cDNA loading on the MNP (each conjugated to several hundred copies of cDNAs, only one is shown here for simplicity) is used to enhance T-DNA capture efficiency and binding affinity.[14] Moreover, we have previously found that MNP-immobilized enzymes retained much higher activities over those on flat surfaces (~5-fold) from improved substrate accessibility.[15] All these lead to significantly improved sensitivity. After magnetic separation, followed by washing steps, Amplex red and fluorescein diphosphate (FDP), which can be efficiently turned over by HRP and ALP into resorufin (λ_{max} = 571 nm) and fluorescein (λ_{max} = 485 nm), respectively, are added simultaneously. This allows the HRP/ALP-catalyzed reactions to be used for T-DNA1/T-DNA2 detection, respectively.

Enzyme Activity and Termination. This assay uses specific colored products generated by HRP/ALP-catalyzed reactions for T-DNA1/T-DNA2 detection. It is useful to be able to terminate the enzymatic reaction after a certain amplifying period before measurement. Here, NaN_3 and PBS are found to effectively stop the HRP- and ALP-catalyzed reactions, respectively (Supporting Information, Figure S1). Moreover, the substrate turnover rate (TR) for HRP−NAV and ALP−NAV can be estimated from the assay slopes and ε of resorufin (54 000 $M^{-1}\cdot cm^{-1}$) and fluorescein (50 400 $M^{-1}\cdot cm^{-1}$) via TR = slope/([enzyme]ε). This yields TRs of 65 s^{-1} in PBS and 56 s^{-1} in Tris buffer for HRP−NAV, and 65 s^{-1} for ALP−NAV in Tris, consistent with the literature.[15]

Characterization of MNP and MNP−NH_2. The MNP is found to be mainly made of magnetite from the X-ray diffraction (Fe_3O_4, Supporting Information, Figure S2A). A strong IR absorption at ~569 cm^{-1}, corresponding to the ν_{Fe-O} of the magnetite core,[16] is found in both the MNP/MNP−NH_2 (Supporting Information, Figure S2B). A new band at ~1085 cm^{-1} in the MNP−NH_2 maybe assigned to the ν_{Si-O} of the silica shell. In addition, a broad band at ~3440 cm^{-1} in the MNP−NH_2 may be assigned to ν_{N-H} or ν_{O-H}. These results are consistent with the MNP being successfully coated with an aminenated silica shell. Hydrodynamic diameters (HDs) of the MNP and MNP−NH_2 were measured as 28.9 ± 5.3 and 178 ± 26 nm, respectively, by dynamic light scattering[17] (Supporting Information, Figure S2C). The MNP−NH_2 shows no apparent hysteresis with a saturated magnetization of ~40 emu/g in its magnetization curve (Supporting Information, Figure S2D), lower than the MNP core (ca. ~90 emu/g),[15a] but is consistent with the coating of a nonmagnetic shell. This confirms the MNP−NH_2 is superparamagnetic and well-suited for biosensing: they form a stable, uniform dispersion in water but can be rapidly retrieved (1 min) with a magnet (Supporting Information, Figure S3).

Assay Optimization. A series of experiments are performed to optimize this assay.

First, MNP Surface Passivation. The MNP−NH_2 was first reacted with excess $SM(PEG)_{12}$ to introduce maleimides for cDNA conjugation, where any unreacted maleimides on the MNP could lead to nonspecific enzyme adsorption and increasing background. A treatment with 2-mercaptoethanol (to cap unreacted maleimides) followed by bovine serum albumin blocking (1 mg/mL) was found highly effective, leading to a greatly improved signal to background (S/B) ratio (from ~4.4 to ~62, Supporting Information Figure S4A).

Second, Amount of MNP−cDNA. Despite of surface passivation, this cannot eliminate nonspecific adsorption of enzymes on the MNPs completely. Supporting Information Figure S4B showed assay signal increased with the increasing amount of MNP−cDNA1, indicating more efficient T-DNA capture; however, the background also increased. As a result,

dx.doi.org/10.1021/ac402081u | Anal. Chem. 2013, 85, 9238−9244

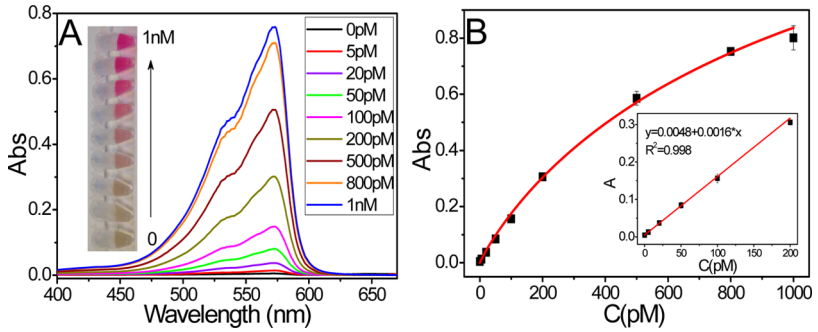

Figure 1. (A) Absorption spectra of the assay samples with different amounts of T-DNA1 using 1 h amplification. Inset: a photograph of the corresponding samples. (B) The resulting calibration curve for T-DNA1 quantification. Inset: amplified region over the 0−200 pM T-DNA1 range fitted to a linear function.

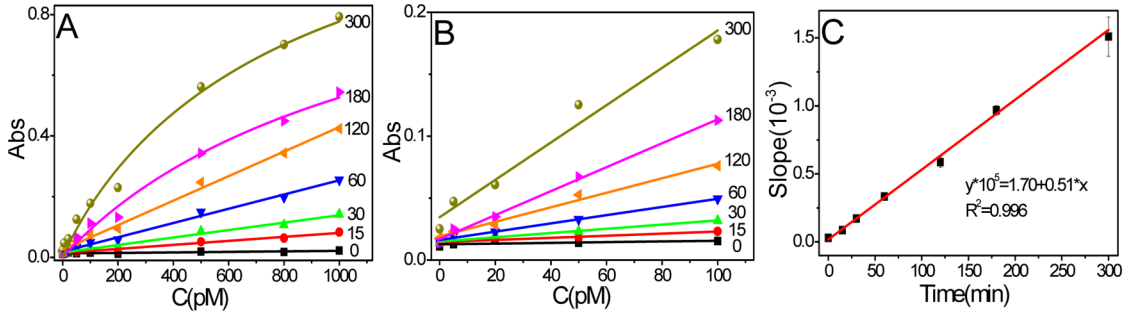

Figure 2. (A) Calibration curves for T-DNA1 quantitation using different enzymatic amplification times (0−300 min; the amplification times are indicated on each curve). (B) The amplified region over the 0−100 pM T-DNA1 range, and data were fitted to linear relationships. (C) The relationship between the corresponding slopes of calibration curves in panel B and the enzymatic amplification times.

the net signal arising from T-DNA1 actually decreased when >20 μg of MNP was used. Therefore, 20 μg MNP−cDNA was used for subsequent colorimetric sensing. Despite giving a weaker net T-DNA1 signal, 10 μg MNP−cDNA actually yielded the highest S/B ratio, so 10 μg MNP was used to assess the detection limit via fluorescence (both enzymatic products are fluorescent).

Third, Temperature. Supporting Information Figure S4C revealed that assay sensitivity was strongly temperature-dependent: a 140% increase of sensitivity was observed as temperature was increased from 4 to 24 °C (~RT) but no further increase was shown as temperature was increased to 37 °C. Hence, all assays were carried out conveniently at RT.[19]

Fourth, cDNA Loading. Increasing the cDNA loading on the MNP can increase the affinity and amount of cDNAs available for T-DNA hybridization, and hence may increase capture efficiency. Figure S4D (Supporting Information) shows that the sensitivity increases first with the increasing cDNA loading, reaching the maximum value at ~0.5 nmol/mg (MNP). This loading was used for all subsequent assays.

DNA1 Quantitation Using HRP-Based Signal Amplification. The optimized conditions were used to quantitate T-DNA1 using MNP−cDNA1/HRP−sDNA1. Figure 1 shows the absorption spectra of assay samples and the resulting calibration curve (1 h amplification). An extremely low background (sample without T-DNA1, A_{571} = 0.0045 ± 0.0003) is observed. The signal is increased greatly with the T-DNA1 concentration, confirming the success of our assay strategy. In fact, the signal at 1 nM T-DNA1 (0.801 ± 0.043) is ~177 times that of the blank, demonstrating an excellent S/B ratio and further confirming the success of our assay optimizations. A high S/B ratio is very beneficial for biosensing, allowing for direct, accurate target quantitation without the need of background correction.

Like typical enzymatic reactions, the whole calibration curve initially displays a rapid linear increase with T-DNA1 concentration up to 200 pM (R^2 = 0.998, Figure 1B inset). As T-DNA1 concentration is increased further, the calibration curve deviates from linear and gradually becomes saturated, due to depleted Amplex red at higher target DNA (hence HRP) concentrations. This overall calibration curve could be fitted well (R^2 = 0.991) by the Hill equation, yielding an apparent k of 394 nM (K_M minic of enzyme activity) and n of 1.06, suggesting no strong target-binding cooperation.

We have evaluated the effect of amplification time on assay sensitivity. As shown in Figure 2, over the whole 0−1 nM range, the calibration curves showed good linearity up to 120 min of amplification time. As amplification time is extended further to >180 min, the calibration curves deviate from linearity, due to depletion of the substrates under such conditions (10 μM Amplex red/H_2O_2). A careful examination of the calibration curves over the 0−100 pM range (Figure 2B) reveals all curves are linear. Besides, the corresponding slopes (representing sensitivity) are found to increase linearly with the amplification time (R^2 = 0.996, Figure 2C), suggesting the sensitivity can be increased by extending the amplification time.

A large and systematically tunable dynamic range is important for biosensing. Here, we show that the amplification time can be used to tune the dynamic range and sensitivity: the dynamic range can be enlarged by reducing amplification time, while increasing the amplification time can be used to improve assay sensitivity. For example, by extending the amplification time from 1 h to overnight (~15 h), this assay can directly

dx.doi.org/10.1021/ac402081u | *Anal. Chem.* 2013, 85, 9238−9244

detect 100 fM T-DNA unambiguously by UV−vis spectra with a good linearity over the 0−10 pM range (R^2 =0.990, Figure 3).

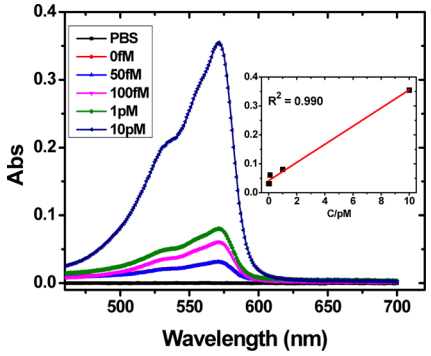

Figure 3. Absorption spectra of samples containing different amounts of T-DNA3 detected by MNP−cDNA3 and HRP−sDNA3 with overnight amplification. Inset: calibration curve with linear fit; y = 0.0417 + 0.0314x, R^2 = 0.990.

Moreover, by adapting a more sensitive readout using a conventional fluorescence plate reader,[18] this assay can detect 50 fM T-DNA3 directly without target preamplification over 2 h (Supporting Information, Figure S5). Such a sensitivity is higher than many other sensitive, direct DNA sensing techniques, e.g., GNP-amplified surface plasmon resonance (~10 pM),[20] microcantilever-based nanomechanical sensing (~10 pM),[21] electrochemical DNA sensing (10−50 pM),[22] enzyme-amplified electrochemical DNA sensing with a DNA tetrahedron (1 pM),[23] and silver nanoparticle amplified surface-enhanced Raman scattering (1.1−33 pM).[24] It is also comparable to some ultrasensitive DNA assays, e.g., silver-amplified GNP−DNA-based scannometric assay/electric detection (~50 fM),[4,5] electrochemical DNA sensing via enzymatic amplification (~10 fM),[22a] or via a DNA super-sandwich assembly (~100 fM).[22c] Another advantage here is that the MNP−target−En sandwiches can be easily retrieved magnetically, allowing MNP-bound species to be concentrated or diluted where required, which can be further combined with the tuning of amplification time to achieve the most desirable dynamic range and sensitivity for each specific assay needs.

The ability to perform assays in complex, clinical media is important for real-world applications. To demonstrate this potential, T-DNA1 detection was carried out in 10% human serum (a clinical media, 1 h amplification). Figure S6 (Supporting Information) reveals the T-DNA1 detection is unaffected in 10% human serum, yielding a good linear calibration curve (R^2 = 0.999). This demonstrates the MNP−enzyme assay is highly robust and works efficiently in complex media. We attribute this to the careful management of the MNP surfaces and assay conditions, leading to greatly reduced background and excellent assay robustness.

Stability of MNP−cDNA probe is another important parameter. Here we have performed T-DNA detection using MNP−cDNA probes after being stored for up to 5 months at 4 °C in pure water and compared the result with the fresh probes. Results show that not only have the 5 month old MNP−cDNA probes remained magnetically responsive, but they also give similar sensitivities (calibration slopes) to the fresh MNP−cDNA (Supporting Information, Figure S7), confirming the MNP−cDNA probe has good long-term stability.

T-DNA2 Detection Using ALP-Based Signal Amplification. The ALP-catalyzed turnover of FDP into fluorescein (λ_{max} = 485 nm) was used to detect T-DNA2 using MNP−cDNA2 and ALP−sDNA2 probes. The assay was done in Tris buffer because PBS inhibits the ALP activity (Supporting Information Figure S1).[26] The resulting absorption spectra of assay samples (1 h amplification) and the corresponding calibration curve are shown in Figure 4. A good positive linear calibration curve (R^2 = 0.994) over the 0−200 pM range is obtained, suggesting that ALP is just as powerful as HRP in signal amplification, allowing direct quantitation of low picomole per liter T-DNA2 with 1 h amplification.

Simultaneous Quantification of Two T-DNAs. The ability to simultaneously detect two or more DNA targets is important for high clinical diagnostic accuracy.[10] To demonstrate this potential, two sets of MNP−cDNA and En−sDNA probes are used to detect two specific T-DNAs via HRP- and ALP-catalyzed reactions, respectively (Scheme 1).

Figure 5A shows the absorbance of both resorufin (A_{571}) and fluorescein (A_{485}) increased significantly with the increasing T-DNA1/T-DNA2 concentration (1 h amplification). Moreover, the correlations between the absorbance and T-DNA concentrations are both linear (R^2 = 0.975 for T-DNA1 and 0.994 for T-DNA2) over the 0−500 pM range (Figure 5B). Interestingly, both plots yield very similar slopes (sensitivities), in agreement with their similar substrate turnover rates.

These results thus established a simple, general, and versatile doublet DNA assay that can be applied to target any DNA of

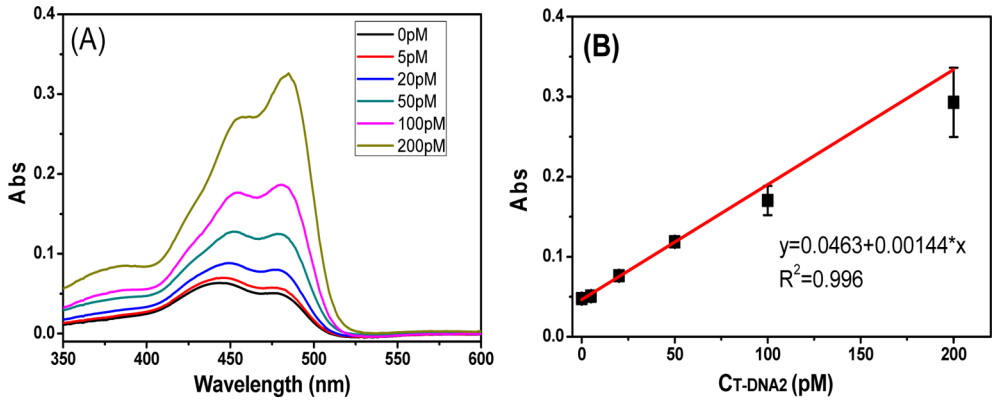

Figure 4. (A) UV−vis absorption spectra of assay samples with different concentrations of T-DNA2 using ALP-based signal amplification. (B) The corresponding A_{485} vs concentration relationship of the assays and corresponding linear fit (red line).

dx.doi.org/10.1021/ac402081u | Anal. Chem. 2013, 85, 9238−9244

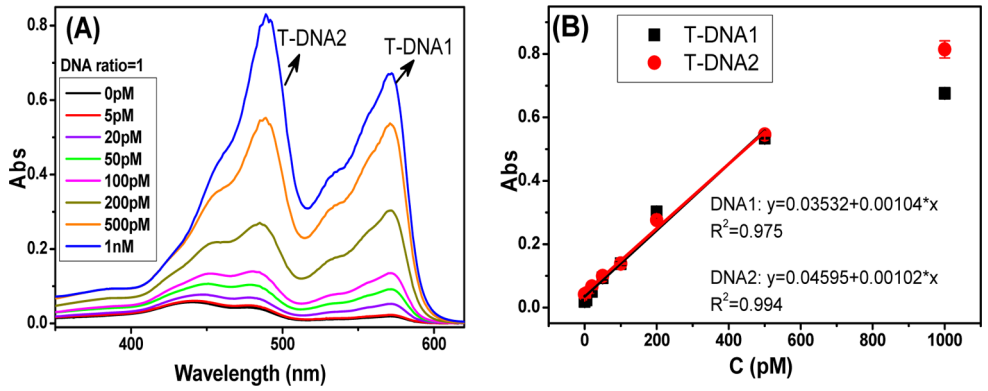

Figure 5. Simultaneous quantification of two DNA targets using the MNP–enzyme sandwich assay. (A) Absorption spectra of the assay samples with different amounts of T-DNAs; T-DNA1/T-DNA2 molar ratio = 1:1. (B) The corresponding calibration curves for both DNA targets: data within the 0–500 pM range were both fitted to linear functions.

interest by designing a pair of unique MNP–cDNA and En–sDNA probes for each specific T-DNA. Additional advantages here include (1) the use of MNP-based homogeneous, rapid target capture, (2) convenient magnetic separation for low assay background, and (3) the use of large excesses of MNP–cDNA/En–sDNA probes to push T-DNA hybridization equilibrium toward the captured state, allowing efficient capture and detection of T-DNA at concentrations well below the corresponding K_d.[2,7,8] As a result, this simple DNA assay can offer superior sensitivity and specificity over many other more established DNA sensing methods (see Supporting Information Table S1) and appears well-suited for broad DNA-based biosensing and diagnostics.

Discrimination of Cancer-Specific Single-Base Mutation. Genetic single-nucleotide polymorphism (SNP) is associated with numerous human diseases, e.g., cancer, diabetes, vascular disease, and some forms of mental illness.[28,29] To demonstrate the potential of our assay in SNP discrimination, the KRAS mutations (codon 12/13) associated with several human cancers, e.g., colorectal,[30] pancreas,[31] and lung,[32] are chosen as the DNA targets. This involves three T-DNAs (Table 1), the wild-type (T-DNA3) and two cancer-specific SNPs, T-DNA4 (17*C* → *T*) and T-DNA5 (17*C* → *A*). Here MNP–cDNA3 and HRP–sDNA3, fully complementary to T-DNA3, are used ($C_{T\text{-}DNA}$ = 100 pM, 1 h amplification). Figure 6 shows that the signal of the full-match T-DNA3 is considerably higher than the two cancer-specific SNPs, confirming this assay can distinguish the normal gene from cancer-specific SNP mutants. The discrimination ratios (DRs) obtained here are 2.1 and 2.5 for T-DNA3/T-DNA4 and T-DNA3/T-DNA5 pairs, respectively. Reducing the assay buffer NaCl content from 150 to 100 mM improves the above SNP DRs to 3.3 and 4.2, respectively (Supporting Information, Figure S8), comparable to many reported DNA SNP assays, presumably because the formed MNP–dsDNA sandwiches containing a single mismatch (with cancer-specific SNPs) are affected more severely than the full-match wide-type target, in agreement with the literature.[27,33] Further reducing the NaCl content to 50 mM produced significantly reduced signals for all T-DNAs (data not shown), due to greatly reduced stability of the dsDNA sandwich structure.

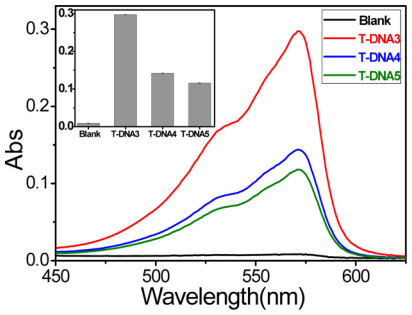

Figure 6. UV–vis spectra of samples showing the discrimination of cancer-specific SNPs (T-DNA4/TDNA5) against the wild-type noncancer gene. Inset: A_{571} values of the DNA targets.

CONCLUSION

In summary, we have successfully developed a simple, sensitive, and general MNP–enzyme sandwich assay that can be used for simultaneous quantitation of two specific DNA targets in clinically relevant media (e.g., 10% human serum). By combining the MNP-based rapid, efficient target capture and convenient magnetic separation and enzyme-based great signal amplification together with the careful optimization of the MNP surface and assay conditions, this assay can achieve direct, label-free quantitation of T-DNA down to 50 fM level with a total assay time of <3 h (via fluorescence readout). Such a sensing performance places it among the very best of PCR- and label-free DNA assays in terms of both sensitivity and specificity (Supporting Information Table S1).[15,34] Moreover, this assay is highly specific: it can effectively discriminate between a normal KRAS gene from its two cancer-specific SNPs. Therefore, we believe this robust, general, sensitive DNA sensing technology should have great potential in a wide range of DNA-based biosensing and diagnostic applications. Currently, we are focused on further improving the assay sensitivity and SNP discrimination ratio and extending its application to clinical samples.

ASSOCIATED CONTENT

Supporting Information

Experimental details on MNP synthesis, surface modification, cDNA conjugation, and surface passivation as well as detailed assay procedures and supporting figures. This material is available free of charge via the Internet at http://pubs.acs.org.

dx.doi.org/10.1021/ac402081u | *Anal. Chem.* 2013, 85, 9238–9244

AUTHOR INFORMATION

Corresponding Authors

*E-mail: y.guo@leeds.ac.uk. Phone: +44-113-3436230. Fax: +44-113-3436565.

*E-mail: d.zhou@leeds.ac.uk. Phone: +44-113-3436230. Fax: +44-113-3436565.

Present Address

[‖]Laboratory of Physical Chemistry, Molecular and Cellular Biology, Center of Excellence for Molecular Imaging (CEMI), Department of Radiologic Technology, Faculty of Associated Medical Sciences, Chiang Mai University, Chiang Mai, 50200 Thailand.

Notes

The authors declare no competing financial interest.

ACKNOWLEDGMENTS

We thank the Leeds Biomedical Health Research Centre, Leeds Cancer Research U.K. Centre, and University of Leeds for funding this project. Y.Z. thanks the China Scholarship Council (CSC) and University of Leeds for providing a Ph.D. research scholarship. Y.G. thanks the Wellcome Trust (U.K.) for providing a Career Re-entry Fellowship (Grant No: 097354/Z/11/Z). P.Q. thanks the Yorkshire Cancer Research and the NIHR/CRUK Experimental Cancer Medicine Centre for supporting his research.

REFERENCES

(1) Song, S.; Liang, Z.; Zhang, J.; Wang, L.; Li, G.; Fan, C. *Angew. Chem., Int. Ed.* **2009**, *48*, 8670−8674.

(2) (a) Giljohann, D. A.; Mirkin, C. A. *Nature* **2009**, *462*, 461−464. (b) Rosi, R. L.; Mirkin, C. A. *Chem. Rev.* **2005**, *105*, 1547−1562.

(3) (a) Köppel, R.; Ruf, J.; Rentsch, J. *Eur. Food Res. Technol.* **2011**, *232*, 151−155. (b) Yamashige, R.; Kimoto, M.; Mitsui, T.; Yokoyama, S.; Hirao, I. *Org. Biomol. Chem.* **2011**, *9*, 7504−7509.

(4) Taton, T. A.; Mirkin, C. A.; Letsinger, R. L. *Science* **2000**, *289*, 1757−1760.

(5) Park, S. J.; Taton, T. A.; Mirkin, C. A. *Science* **2002**, *295*, 1503−1506.

(6) Cao, Y. C.; Jin, R.; Mirkin, C. A. *Science* **2002**, *297*, 1536−1540.

(7) Nam, J. M.; Thaxton, C. S.; Mirkin, C. A. *Science* **2003**, *301*, 1884−1886.

(8) Zhang, Y.; Zhou, D. J. *Expert Rev. Mol. Diagn.* **2012**, *12*, 565−571.

(9) (a) Cass, A. E.; Davis, G.; Francis, G. D.; Hill, H. A. O.; Aston, W. J.; Higgins, I. J.; Plotkin, E. V.; Scott, L. D.; Turner, A. P. *Anal. Chem.* **1984**, *56*, 667−671. (b) Xiao, Y.; Patolsky, F.; Katz, E.; Hainfeld, J. F.; Willner, I. *Science* **2003**, *299*, 1877−1881.

(10) U.S. National Cancer Institute Website. http://www.cancer.gov/cancertopics/factsheet/detection/tumor-markers (accessed June 15, 2013).

(11) Gaster, R. S.; Hall, D. A.; Nielsen, C. H.; Osterfeld, S. J.; Yu, H.; Mach, K. E.; Wilson, R. J.; Murmann, B.; Liao, J. C.; Gambhir, S. S. *Nat. Med.* **2009**, *15*, 1327−1332.

(12) Tyagi, S.; Bratu, D. P.; Kramer, F. R. *Nat. Biotechnol.* **1998**, *16*, 49−53.

(13) (a) He, S.; Song, B.; Li, D.; Zhu, C.; Qi, W.; Wen, Y.; Wang, L.; Song, S.; Fang, H.; Fan, C. *Adv. Funct. Mater.* **2010**, *20*, 453−459. (b) Zhang, M.; Yin, B. C.; Tan, W.; Ye, B. C. *Biosens. Bioelectron.* **2011**, *26*, 3260−3265.

(14) Lytton-Jean, A. K.; Mirkin, C. A. *J. Am. Chem. Soc.* **2005**, *127*, 12754−12755.

(15) (a) Garcia, J.; Zhang, Y.; Taylor, H.; Cespedes, O.; Webb, M. E.; Zhou, D. J. *Nanoscale* **2011**, *3*, 3721−3730. (b) Rauf, S.; Zhou, D. J.; Abell, C.; Klenerman, D.; Kang, D. J. *Chem. Commun.* **2006**, 1711. (c) Kim, D. C.; Sohn, J. I.; Zhou, D. J.; Duke, T. A. J.; Kang, D. J. *ACS Nano* **2010**, *4*, 1580−1586.

(16) (a) Wang, S.; Cao, H.; Gu, F.; Li, C.; Huang, G. *J. Alloys Compd.* **2008**, *457*, 560−564. (b) Kralj, S.; Drofenik, M.; Makovec, D. *J. Nanopart. Res.* **2011**, *13*, 2829−2841.

(17) Song, L.; Ho, V. H.; Chen, C.; Yang, Z.; Liu, D.; Chen, R.; Zhou, D. J. *Adv. Healthcare Mater.* **2013**, *2*, 275−280.

(18) Zhang, Y.; Guo, Y.; Quirke, P.; Zhou, D. J. *Nanoscale* **2013**, *5*, 5027−5035.

(19) Farhangrazi, Z. S.; Fossett, M. E.; Powers, L. S.; Ellis, W. R., Jr. *Biochemistry* **1995**, *34*, 2866−2871.

(20) He, L.; Musick, M. D.; Nicewarner, S. R.; Salinas, F. G.; Benkovic, S. J.; Natan, M. J.; Keating, C. D. *J. Am. Chem. Soc.* **2000**, *122*, 9071−9077.

(21) Zhang, J.; Lang, H.; Huber, F.; Bietsch, A.; Grange, W.; Certa, U.; McKendry, R.; Güntherodt, H.-J.; Hegner, M.; Gerber, C. *Nat. Nanotechnol.* **2006**, *1*, 214−220.

(22) (a) Fan, C.; Plaxco, K. W.; Heeger, A. J. *Proc. Natl. Acad. Sci. U.S.A.* **2003**, *100*, 9134−9137. (b) Rowe, A. A.; Chuh, K. N.; Lubin, A. A.; Miller, E. A.; Cook, B.; Hollis, D.; Plaxco, K. W. *Anal. Chem.* **2011**, *83*, 9462−9466. (c) Xia, F.; White, R. J.; Zuo, X.; Patterson, A.; Xiao, Y.; Kang, D.; Gong, X.; Plaxco, K. W.; Heeger, A. J. *J. Am. Chem. Soc.* **2010**, *132*, 14346−14348.

(23) Pei, H.; Lu, N.; Wen, Y.; Song, S.; Liu, Y.; Yan, H.; Fan, C. *Adv. Mater.* **2010**, *22*, 4754−4758.

(24) Faulds, K.; McKenzie, F.; Smith, W. E.; Graham, D. *Angew. Chem., Int. Ed.* **2007**, *46*, 1829−1831.

(25) (a) Prime, K. L.; Whitesides, G. M. *J. Am. Chem. Soc.* **1993**, *115*, 10714−10721. (b) Zhou, D.; Bruckbauer, A.; Ying, L.; Abell, C.; Klenerman, D. *Nano Lett.* **2003**, *3*, 1517−1520. (c) Zhou, D. J.; Bruckbauer, A.; Abell, C.; Klenerman, D.; Kang, D. J. *Adv. Mater.* **2005**, *17*, 1243−1248.

(26) Hill, H. D.; Summer, G. K.; Waters, M. D. *Anal. Biochem.* **1968**, *24*, 9−17.

(27) (a) Patolsky, F.; Weizmann, Y.; Katz, E.; Willner, I. *Angew. Chem., Int. Ed.* **2003**, *42*, 2372−2376. (b) Bi, S.; Li, L.; Zhang, S. *Anal. Chem.* **2010**, *82*, 9447−9454. (c) Shi, C.; Ge, Y.; Gu, H.; Ma, C. *Biosens. Bioelectron.* **2011**, *26*, 4697−4701. (d) Chen, X.; Ying, A.; Gao, Z. *Biosens. Bioelectron.* **2012**, *36*, 89−94.

(28) Xue, X.; Xu, W.; Wang, F.; Liu, X. *J. Am. Chem. Soc.* **2009**, *131*, 11668−11669.

(29) (a) Wang, Y.; Li, C.; Li, X.; Li, Y.; Kraatz, H. B. *Anal. Chem.* **2008**, *80*, 2255−2260. (b) Hacia, J. G.; Brody, L. C.; Chee, M. S.; Fodor, S. P. A.; Collins, F. S. *Nat. Genet.* **1996**, *14*, 441−447. (c) Santiago, F. S.; Todd, A. V.; Hawkins, N. J.; Ward, R. L. *Mol. Cell. Probes* **1997**, *11*, 33−38. (d) Halushka, M. K.; Fan, J. B.; Bentley, K.; Hsie, L.; Shen, N.; Weder, A.; Cooper, R.; Lipshutz, R.; Chakravarti, A. *Nat. Genet.* **1999**, *22*, 239−247. (e) Duan, X.; Li, Z.; He, F.; Wang, S. *J. Am. Chem. Soc.* **2007**, *129*, 4154−4155.

(30) Lievre, A.; Bachet, J.-B.; Le Corre, D.; Boige, V.; Landi, B.; Emile, J.-F.; Côté, J.-F.; Tomasic, G.; Penna, C.; Ducreux, M. *Cancer Res.* **2006**, *66*, 3992−3995.

(31) Almoguera, C.; Shibata, D.; Forrester, K.; Martin, J.; Arnheim, N.; Perucho, M. *Cell* **1988**, *53*, 549−554.

(32) San Tam, I. Y.; Chung, L. P.; Suen, W. S.; Wang, E.; Wong, M. C.; Ho, K. K.; Lam, W. K.; Chiu, S. W.; Girard, L.; Minna, J. D. *Clin. Cancer Res.* **2006**, *12*, 1647−1653.

(33) Gerion, D.; Chen, F.; Kannan, B.; Fu, A.; Parak, W. J.; Chen, D. J.; Majumdar, A.; Alivisatos, A. P. *Anal. Chem.* **2003**, *75*, 4766−4772.

(34) Hu, J.; Zhao, X. W.; Zhao, Y. J.; Li, J.; Xu, W. Y.; Wen, Z. Y.; Xu, M.; Gu, Z. Z. *J. Mater. Chem.* **2009**, *19*, 5730−5736.